DALTON
FULL PAPER

# Divalent first-row transition metal complexes of the rigid pendant-arm ligand 1,4,7-tris(2-aminophenyl)-1,4,7-triazacyclononane †

**Ian A. Fallis,* Richard D. Farley, K. M. Abdul Malik, Damien M. Murphy and Hayley J. Smith**

*Department of Chemistry, Cardiff University, PO Box 912, Cardiff, UK CF10 3TB*

***Received 5th July 2000, Accepted 6th September 2000***
***First published as an Advance Article on the web 3rd October 2000***

The rigid pendant-arm macrocyclic ligand 1,4,7-tris(2-aminophenyl)-1,4,7-triazacyclononane ($L^1$) has been synthesized. It reacts with divalent first row transition metal perchlorate salts to yield complexes of general formula $[M^{II}(L^1)][ClO_4]_2$ (M = $Fe^{II}$, $Ni^{II}$, $Cu^{II}$ or $Zn^{II}$). Single crystal X-ray crystallography indicated that $[Fe^{II}(L^1)][ClO_4]_2$ and $[Ni^{II}(L^1)][ClO_4]_2$ are isostructural with both complex cations consisting of distorted pseudo-octahedral six-co-ordinate metal centres with three macrocyclic *N*-donors and three anilino donors. The mean Fe–N bond length in $[Fe^{II}(L^1)][ClO_4]_2$ was found to be 2.10 Å, which is intermediate between the normal ranges of high and low spin $Fe^{II}N_6$ species. Magnetometry and EPR measurements indicated that single crystals of $[Fe^{II}(L^1)][ClO_4]_2$ were predominately low spin, with approximately 5% of a low spin iron(III) species present in the lattice. It is postulated that this latter species is the mono anilido complex $[Fe^{III}(L^{1-H})][ClO_4]_2$. The crystal structure of $[Ni^{II}(L^1)][ClO_4]_2$ indicated a short mean Ni–N bond length of 2.09 Å. The ligand field strength for this material was found to have a very high value of 12,330 $cm^{-1}$ ($B$ = 850 $cm^{-1}$) and is compared to that of some related trigonal $Ni^{II}N_6$ species. The crystal structure of $[Cu^{II}(L^1)][ClO_4]_2$ was also determined and indicated a distorted six-co-ordinate metal centre. The X-band EPR spectrum of this complex in magnetically dilute solid solution indicated a predominantly axial species, although a slight rhombic distortion may be present. The variable temperature $^1H$ NMR of $[Zn^{II}(L^1)][ClO_4]_2$ in $CD_3CN$ solution revealed a non-fluxional six-co-ordinate complex. Electrochemical analyses of the complexes indicated only irreversible oxidation and reduction processes for $[Ni^{II}(L^1)][ClO_4]_2$ and $[Cu^{II}(L^1)][ClO_4]_2$. $[Fe^{II}(L^1)][ClO_4]_2$ displays at least two reversible oxidation processes with the first at +0.181 V (*vs.* $Fc–Fc^+$) being assigned as a metal centred $Fe^{II} \longrightarrow Fe^{III}$ process and the second at +0.475 V as a ligand centred process.

## Introduction

The synthesis of rigid pendant-arm derivatives of aza-macrocyclic ligands provides a useful means of controlling the ligand environment about transition metal ions.[1] In recent years Wieghardt and co-workers have described the synthesis and co-ordination chemistry of a 1,4,7-triazacyclonane (tacn) based macrocyclic ligand bearing pendant anilino donors (ligand structure L).[2] In L the pendant donor group, as with most pendant-arm donor systems, is linked to the macrocyclic donors *via* a methylene group which imparts a high degree of ligand conformational flexibility. We felt it would be interesting to examine the effect of attaching aniline donor groups directly to the macrocyclic secondary amine positions. Not only would this make the ligand more rigid but would also be expected to increase the strength of metal–ligand interactions by reducing the size of the pendant chelate rings from 6 to 5 membered. To this end we have devised a simple synthesis of the rigid pendant-arm ligand 1,4,7-tris(2-aminophenyl)-1,4,7-triazacyclonane ($L^1$) and have begun to explore its transition metal co-ordination chemistry. To the best of our knowledge $L^1$ represents the first example of an *N*-aryl triazacyclononane derivative. Two examples of tetraaza-macrocyclic ligands bearing *N*-aryl substituents have been reported with Kimura and co-workers describing the preparation and complexation properties of 1-(2,4-dinitrophenyl)-1,4,7,10-tetraazacyclododecane[3] and Collins and co-workers examining the spectroscopic properties of 4-(1,4,8,11-tetraazacyclotetradec-1-yl)benzonitrile.[4] In both these cases however the aryl group does not participate in co-ordination, but acts as a sensitiser or a reporter moiety for spectroscopic measurements. There are of course many examples of triazacyclononane derivatives with pendant anilines, phenols, benzenethiols and heterocyclic donors, but in all these ligand types the aromatic functionalities are bound to the ring nitrogen donors *via* methylene linkages, which confer considerable conformational flexibility upon these systems.[5] We wish to compare these ligands to systems in which aromatic pendant donor groups were linked directly to the macrocycle.

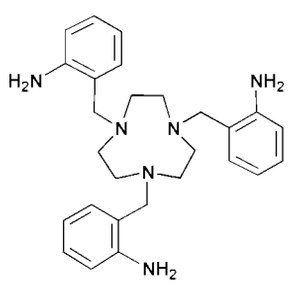


L

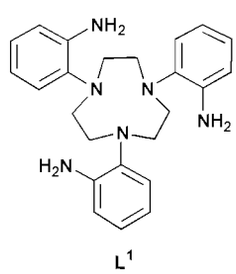


$L^1$

† Electronic supplementary information (ESI) available: X-band EPR spectra of $[FeL^1][ClO_4]_2$ and electronic spectra of nickel(II) complexes. See http://www.rsc.org/suppdata/dt/b0/b005402j/

 DOI: 10.1039/b005402j

$L^1$ also represents an example of an *N*,*N*-disubstituted *o*-phenylenediamine ligand. *ortho N*-Substituted aromatics are of interest due to their 'non-innocent' acid–base and redox behaviour upon co-ordination.[6] There are remarkably few well defined complexes of *o*-phenylenediamine itself[7] although a cobalt(III) templated synthesis of a 21-membered macrocyclic (tribenzo-1,4,8,11,15,18-hexaazacyclohenicosane) containing alternating phenylene and propane bridges derivative has been reported.[8] This paper reports the first examples of structurally characterised tris chelates containing the phenylenediamine moiety.

## Experimental

**CAUTION!** On one occasion a small sample of a metal perchlorate salt of $L^1$ detonated whilst being manipulated as a dry solid. In a separate incident a sample of the ligand monohydroperchlorate salt ($[HL^1][ClO_4]$) exploded under similar circumstances. Whilst no damage or injury was incurred in these incidents it is recommended that perchlorates be prepared and manipulated in very small quantities.

1,4,7-Triazacyclonane was prepared by standard methods[9] and purified (twice) by bulb-to-bulb distillation prior to use. All other reagents (Aldrich) were used as received. Solvents were purified by standard literature methods.[10] All metal complexes were prepared under a nitrogen atmosphere using standard Schlenk techniques. Mass spectra were obtained in FAB (Fast Atom Bombardment) mode in a 3-nitrobenzyl alcohol matrix, IR spectra in KBr discs using a Nicolet 510 series spectrometer and electronic spectra in acetonitrile solution using Perkin-Elmer Lambda 20 or Lambda 900 spectrophotometers. Electrochemical measurements were performed using a Windsor Scientific Eco Chemie Autolab PGSTAT12 potentiometer equipped with a cell consisting of a platinum disc (3 mm) working electrode, a platinum wire counter electrode and a non-aqueous 0.01 M $AgNO_3$–Ag–0.1 M $Bu_4NPF_6$–$CH_3CN$–glass frit reference electrode. All electrochemical measurements were performed in $Bu_4NPF_6$ (0.1 M) supporting electrolyte under an argon atmosphere and the data were analysed using the Eco Chemie GPES suite of software (v. 4.7). Electrochemical potentials are quoted with reference to a ferrocene–ferrocenium internal standard. NMR spectra were obtained on Brüker Avance AMX 400 or JEOL Eclipse 300 spectrometers and referenced to external TMS. EPR spectra were recorded on a Brüker ESP 300-E X-band spectrometer. The *g* values were determined using a Brüker NMR gaussmeter calibrated using the perylene radical anion generated in concentrated sulfuric acid, $g = 2.002569$.

### Preparations

**1,4,7-Tris(2-nitrophenyl)-1,4,7-triazacyclononane (L′).** *Method A.* To a solution of 1,4,7-triazacyclononane (1.29 g, 10 mmol) in dry acetonitrile (100 ml) was added 2-fluoronitrobenzene (4.23 g, 30 mmol) and finely ground potassium carbonate (4.14 g, 30 mmol). The reaction mixture was refluxed under a nitrogen atmosphere for 8 hours and subsequently filtered, whilst hot, through a fluted filter paper. The residual solid was washed with dichloromethane (2 × 50 ml) and the combined acetonitrile filtrate and dichloromethane washings were evaporated to dryness to yield a bright orange solid. This material was purified by washing with several portions of warm ethanol. Yield 3.52 g (72%). $^1$H NMR ($CDCl_3$): $\delta$ 7.53 (d, 3 H, Ar), 7.33 (m, 3 H, Ar), 7.08 (d, 3 H, Ar), 6.88 (m, 3 H, Ar) and 3.46 (s, 12 H, $CH_2$ of macrocycle). $^{13}$C NMR ($CDCl_3$): $\delta$ 145.1 (C of Ar), 143.3 (C of Ar), 133.6 (CH of Ar), 126.3 (CH of Ar), 122.3 (CH of Ar), 121.2 (CH of Ar) and 55.2 ($CH_2$ of macrocycle). IR (KBr disc, cm$^{-1}$): 3052, 2920, 1610, 1561, 1513, 1480, 1435, 1339, 1297, 1255, 1240, 1221, 1178, 732 and 707. Calc. for $C_{24}H_{24}N_6O_6$: C, 58.5; H, 4.9; N, 17.1%. Found: C, 58.6; H, 4.8; N, 17.0%. Mass spectrum: molecular ion peak at *m*/*z* 492 (calc. 492.49).

*Method B.* To a solution of 1,4,7-triazacyclononane trihydrobromide (1 g, 2.7 mmol) in water (5 ml) was added sodium hydroxide (0.645 g, 16.1 mmol). 2-Fluoronitrobenzene (1.14 g, 8 mmol) dissolved in 5 ml of dichloromethane was added and the resulting two phase reaction mixture stirred vigorously overnight. The orange organic layer was separated, diluted with dichloromethane and washed with water, $NaHCO_3$ (sat.) and water. The organic phase was dried ($MgSO_4$) and the solvent removed to afford a bright orange solid. This material was purified by entrainment with several portions of warm ethanol. Yield 0.78 g (59%). This material had identical properties to that prepared by method A.

**1,4,7-Tris(2-aminophenyl)-1,4,7-triazacyclononane ($L^1$).** To a solution of 1,4,7-tris(2-nitrophenyl)-1,4,7-triazacyclonane (1 g, 2 mmol) in tetrahydrofuran–ethanol (10 : 1, 100 ml) was added palladium (10%) on carbon (100 mg). Hydrogen was bubbled through the stirred reaction mixture for 20 hours during which a fresh portion of catalyst was added. The reaction was filtered under nitrogen through a pad of Celite and the solvent removed under reduced pressure. The residue was recrystallised from a small volume of hot oxygen-free ethanol to afford the required product as an off-white crystalline solid. Yield 0.51 g (62%). $^1$H NMR (400 MHz, $CDCl_3$): $\delta$ 6.97 (d, 3 H, Ar), 6.78 (t, 3 H, Ar), 6.60 (m, 6 H, Ar), 4.17 (s (br), 6 H, $NH_2$) and 3.39 (12 H, s, $CH_2$ of macrocycle). $^1$H NMR (300 MHz, $CD_3CN$): $\delta$ 6.97 (d, 3 H, Ar), 6.78 (t, 3 H, Ar), 6.60 (m, 6 H, Ar), 4.17 (s (br), 6 H, $NH_2$) and 3.39 (12 H, s, $CH_2$ of macrocycle). $^{13}$C NMR (100 MHz, $CDCl_3$): $\delta$ 141.3 (C of Ar), 140.4 (C of Ar), 123.8 (CH of Ar), 122.1 (CH of Ar), 117.6 (CH of Ar) and 114.6 (CH of Ar). IR (KBr disc, cm$^{-1}$) 3449, 3331, 3045, 2854, 2822, 1606, 1497, 1452, 1374, 1318, 1300, 1149, 1129, 1042, 745 and 611. Calc. for $C_{24}H_{30}N_6$: C, 71.6; H, 7.5; N, 20.9%. Found: C, 71.4; H, 7.3; N, 20.7%. Mass spectrum: molecular ion peak at *m*/*z* 402 (calc. 402.54).

**$[Fe^{II}(L^1)][ClO_4]_2$ 1.** To suspension of $L^1$ (40 mg, 0.1 mmol) in thoroughly degassed ethanol (20 ml) was added an excess of $Fe(ClO_4)_2 \cdot 6H_2O$ (40 mg, 1.1 mmol). The reaction mixture was slowly heated to reflux during which time the ligand dissolved to precipitate pale blue micro-crystals. Removal of the supernatant by cannula and subsequent drying *in vacuo* afforded the required complex (59 mg, 90%) as small faintly blue crystals. Crystals of X-ray quality were grown by dissolving this material in hot thoroughly degassed ethanol (60 ml) and allowing the solution to cool slowly and stand for several weeks at room temperature. IR (KBr disc, cm$^{-1}$): 3287, 3240, 3163, 2971, 2943, 1615, 1568, 1497, 1477, 1455, 1280, 1260, 1090, 920, 808, 769, 737, 709, 625, 572 and 455. UV/vis (MeCN, nm): 710. Calc. for $C_{24}H_{30}Cl_2FeN_6O_8$: C, 43.9; H, 4.6; N, 12.8%. Found: C, 44.0; H, 4.7; N, 12.9%.

**$[Ni^{II}(L^1)][ClO_4]_2$ 2.** This material was prepared in a similar manner to that of **1** by treating $L^1$ (40 mg, 0.1 mmol) with an excess of $Ni(ClO_4)_2 \cdot 6H_2O$ (40 mg, 1.1 mmol). Yield 59 mg (90%) of a pink crystalline powder. Crystals of X-ray quality were grown by dissolving this material in hot degassed ethanol (40 ml) and allowing the solution to cool slowly and stand for several days at room temperature. IR (KBr disc, cm$^{-1}$): 3315, 3264, 3179, 2872, 1619, 1575, 1495, 1478, 1455, 1278, 1231, 1092, 947, 931, 920, 900, 810, 770, 734, 714, 621, 595, 576, 556 and 457. UV/vis (MeCN, nm ($\varepsilon$/dm$^3$ mol$^{-1}$ cm$^{-1}$)): 869 (sh) (13), 811 (17), 521 (11) and 326 (sh) (26). Calc. for $C_{24}H_{30}Cl_2N_6NiO_8$: C, 43.7; H, 4.6; N, 12.7%. Found: C, 43.4; H, 4.8; N, 12.0%.

**$[Cu^{II}(L^1)][ClO_4]_2 \cdot EtOH$ 3.** The method used to prepare this material was analogous to that for **1** using 40 mg of $Cu(ClO_4)_2 \cdot 6H_2O$. Yield 48 mg (68%). UV/vis (MeCN, nm ($\varepsilon$/dm$^3$ mol$^{-1}$

$cm^{-1}$)): 695 (103) and 1200 (30). Calc. for $C_{26}H_{36}Cl_2CuN_6O_9$: C, 43.9; H, 5.1; N, 11.8%. Found: C, 43.5; H, 5.3; N, 11.7%. Mass spectrum: molecular ion peak at *m/z* 464.4 (566 {$[Cu^{II}(L^1)][ClO_4]$}$^+$ also observed).

**$[Zn^{II}(L^1)][ClO_4]_2$ 4.** The method used to prepare this material was analogous to that for $[Ni^{II}(L^1)][ClO_4]_2$, using 100 mg (2.5 mmol) of $L^1$ and 100 mg $Zn(ClO_4)_2 \cdot 6H_2O$. Yield 110 mg (66%). $^1$H NMR (400 MHz , $CD_3CN$): $\delta$ 7.57 (d, 3 H, Ar), 7.35 (t, 3 H, Ar), 7.24 (m, 6 H, Ar), 4.56 (s (br), 6 H, $NH_2$), 3.60 (6 H, m, $CH_2$ of macrocycle) and 2.99 (6 H, m, $CH_2$ of macrocycle). $^{13}$C NMR($CD_3CN$): $\delta$ 147.03 (C), 134.05 (C), 129.31 (CH), 128.28 (CH), 127.81 (CH), 125.40 (CH) and 53.62 ($CH_2$). Calc. for $C_{24}H_{30}Cl_2N_6O_8Zn$: C, 43.2; H, 4.5; N, 12.6%. Found: C, 43.0; H, 4.6; N, 12.5%.

**$[Cu^{II}(L^1)][ClO_4]_2$ doped in $[Zn^{II}(L^1)][ClO_4]_2$.** $[Cu^{II}(L^1)][ClO_4]_2 \cdot$ EtOH (5 mg) and $[Zn^{II}(L^1)][ClO_4]_2$ (95 mg) were dissolved in dry oxygen free acetonitrile (1 ml). The resulting suspension was warmed to effect dissolution and cold diethyl ether (5 ml) added to precipitate a grey solid. The supernatant liquid was removed by cannula and the residue washed first with ether (3 ml) and then light petroleum (bp 40–60 °C) (3 ml). The sample was dried *in vacuo* to afford the required product as a blue-grey powder. Yield 84 mg (84%).

### X-Ray crystallography

X-Ray intensity data for the complexes of Fe, Ni and Cu (**1**, **2** and **3** respectively) were collected on a CAD4 diffractometer using monochromated Mo-K$\alpha$ radiation ($\lambda = 0.71073$ Å). Allowances were made for crystal decay for **2** and **3** which, respectively, showed a 24 and 25% fall in the intensities of the standard reflections during the period of data collection. The structures were solved by direct methods (SHELXS 86)[11] and refined on $F^2$ by full-matrix least squares (SHELXL 96)[12] using all unique data. The complexes of Fe and Ni were isostructural; one of the two independent $ClO_4^-$ anions showed orientational disorder with two partially occupied positions for each oxygen atom. The disordered group in both structures was refined with one common Cl–O distance and the anisotropic displacement coefficients of the oxygen atoms constrained to remain 'approximately isotropic' by using an ISOR = 0.012 parameter in SHELXL 96. The copper complex contained an ethanol solvate per complex cation. One O atom of one $ClO_4^-$ anion and the methyl C of the ethanol molecule were refined with an ISOR = 0.015. The non-H atoms in all the structures were anisotropic. The H atoms were included in calculated positions (riding model) with $U_{iso} = nU_{eq}$ ($n = 1.2$ for $NH_2$, $CH_2$ and ring H; 1.5 for $CH_3$ in **3**) of the parent atom. Pertinent crystallographic data, and selected bond distances and angles are given in Tables 1 and 2 respectively.

CCDC reference number 186/2173.

See http://www.rsc.org/suppdata/dt/b0/b005402j/ for crystallographic files in .cif format.

## Results and discussion

### Ligand synthesis and complex preparation

$L^1$ and its complexes are prepared according to reaction Scheme 1. Using method A the initial nucleophilic aromatic substitution reaction of 1,4,7-triazacyclononane with 3 mole equivalents of 2-fluoronitrobenzene in refluxing acetonitrile in the presence of anhydrous potassium carbonate affords the intermediate 1,4,7-tris(2-nitrophenyl)-1,4,7-triazacyclononane (L′) in 72% (isolated) yield. By method B a lower yield was obtained but the synthesis proceeds *via* tacn·3HBr and as such is more convenient. These reactions are not optimised and we are currently investigating a range of different conditions in order to improve yields. Hydrogenation (10% Pd/C, thf–EtOH)

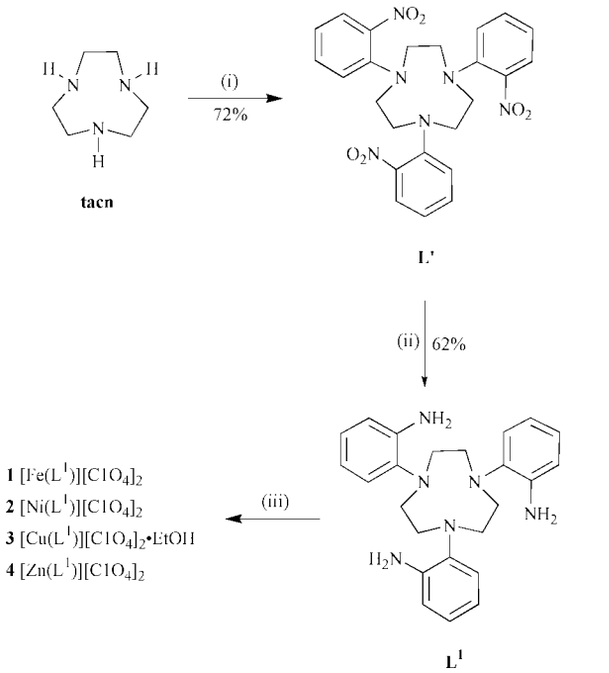


**Scheme 1** *Reagents and conditions*: (i) *o*-$FC_6H_4NO_2$, $K_2CO_3$, MeCN, reflux 8 hours; (ii) 10% Pd/C, $H_2$(g), THF–EtOH; (iii) $M^{II}(ClO_4)_2 \cdot 6H_2O$, EtOH.

and anaerobic work-up of L′ affords $L^1$ in 62% (isolated) yield as a crystalline solid. Solutions of $L^1$ prepared by this method were found rapidly to darken upon exposure to air. Attempts to increase the scale of this reaction resulted in reduced yields and difficult work up procedures. In preparing complexes of $L^1$ it was essential to use anaerobic conditions. For example, solutions of $[Zn^{II}(L^1)][ClO_4]_2$ became red upon exposure to air, although no change in the NMR spectrum of this material was observed. In addition no electrochemical oxidation (0.1 M $Bu_4NPF_6$, MeCN 0–1.5 V *vs*. Fc–Fc$^+$) of this complex or the "free" ligand was observed. We are currently investigating alternative reaction conditions for the hydrogenation step in order to increase the scale and improve the yield of this procedure.

**$[Fe^{II}(L^1)][ClO_4]_2$.** Initial reaction of $L^1$ with $Fe(ClO_4)_2 \cdot 6H_2O$ under anaerobic conditions afforded colourless solutions which upon cooling yielded pale blue micro-crystals of the required product. Recrystallisation of the initial product from ethanol yielded pale blue X-ray quality crystals. The structure of the $[Fe^{II}(L^1)]^{2+}$ cation is shown in Fig. 1 with selected bond lengths and angles collected in Table 2. The complex is monomeric with all six *N*-ligators bound to a distorted octahedral metal centre. The structure as shown is that of the $\Lambda$ isomer in which the macrocyclic chelate rings are of $\delta$ configuration. This material crystallises in a non-enantiomorphous space group, and thus $[Fe^{II}(L^1)][ClO_4]_2$ in the solid state consists of equal quantities of $\Lambda(\delta\delta\delta)$ and $\Delta(\lambda\lambda\lambda)$ cations. An examination of the metal–ligand bond distances indicates a mean Fe–N bond length of 2.10 Å. A selection of $FeN_6$ systems for which crystallographic data are available is collected in Table 3. It can be seen that the mean Fe–N distance is intermediate between typical values observed for high (≈2.20 Å) and low-spin (≈2.00 Å) $Fe^{II}$–$N_6$ systems and is significantly longer than those in iron(III) systems and from the crystallography data alone the assignment of a spin state is somewhat ambiguous.

Ethanolic solutions of complex **1** are very air-sensitive and upon exposure to air rapidly become deep blue with the electronic spectrum indicating a broad, intense band at 710 nm. All attempts at observing a well resolved $^1$H NMR spectrum of the $[Fe^{II}(L^1)]^{2+}$ cation failed. The spectra obtained were broad with

**Table 1** Crystallographic data for complexes **1**, **2** and **3**

| | **1** | **2** | **3** |
|---|---|---|---|
| Chemical formula | $C_{24}H_{30}Cl_2FeN_6O_8$ | $C_{24}H_{30}Cl_2N_6NiO_8$ | $C_{26}H_{36}Cl_2CuN_6O_9$ |
| Formula weight | 657.29 | 660.15 | 711.05 |
| Crystal system | Orthorhombic | Orthorhombic | Triclinic |
| Space group | *Pbca* | *Pbca* | $P\bar{1}$ |
| *a*/Å | 14.298(2) | 14.282(4) | 11.064(6) |
| *b*/Å | 13.759(2) | 13.765(5) | 11.197(4) |
| *c*/Å | 28.230(4) | 28.182(4) | 13.814(7) |
| *α*/° | | | 75.13(3) |
| *β*/° | | | 74.41(4) |
| *γ*/° | | | 67.95(3) |
| *T*/K | 293 | 293 | 293 |
| *Z* | 8 | 8 | 2 |
| $\mu$(Mo-K$\alpha$)/cm$^{-1}$ | 0.795 | 0.953 | 0.966 |
| No. of reflections measured | 5498 | 6316 | 6059 |
| No. of unique data | 4931 | 5618 | 5265 |
| $R_{int}$ | 0.0344 | 0.0650 | 0.0425 |
| *wR*2 (on $F^2$, all data) | 0.1044 | 0.1801 | 0.2153 |
| *R*1 (on, *F*, observed data) | 0.0413 | 0.0672 | 0.0838 |

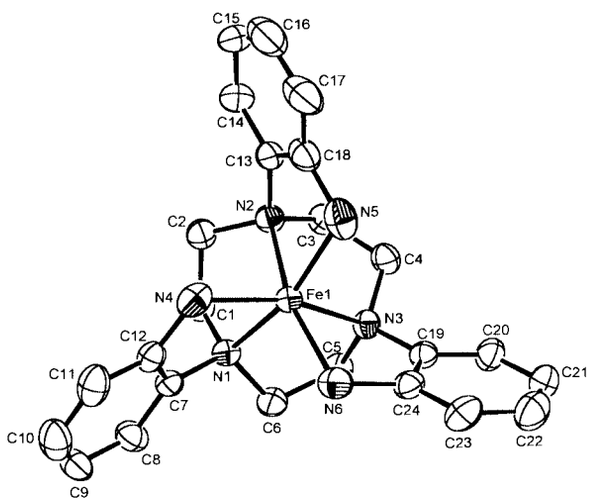


**Fig. 1** Ortep 3[13] plot of $[Fe^{II}(L^1)]^{2+}$ **1** viewed down the approximate 3-fold axis. Ellipsoids are drawn at 40%. Hydrogen atoms are omitted for clarity.

peaks interpreted as macrocyclic ring methylene groups at $\delta$ 2.1 and 2.4 and those for the aryl groups at $\delta$ 11.4 and 14.55. It is believed that the blue coloration observed in the original complex is due to a trace of oxidation of $[Fe^{II}(L^1)]^{2+}$ to the corresponding iron(III) species, the paramagnetism of which results in the broadening of the NMR spectra. Alternatively it is possible that the source of $Fe^{III}$ may be a small impurity in the original iron(II) perchlorate hexahydrate starting material. It was also observed that this oxidation process occurred more slowly in dry acetonitrile solution. The magnetic moment of single crystals of **1** have been measured by variable temperature SQUID magnetometry by Professor Andrew Harrison (University of Edinburgh). This study indicated that **1** contains a low spin iron(II) centre but also that a small (≈5%) quantity of a low-spin iron(III) species was present in the lattice. We also observed that the darkening of solutions of **1** was accelerated by addition of trace amounts of a weak base (*e.g.* triethylamine), which we interpret as a deprotonation of a pendant anilino donor [see ref. 2(c)] to yield a corresponding anilido complex $[Fe^{III}(L^{1-nH})]^{(3-n)+}$. We therefore tentatively suggest that single crystals of **1** contain approximately 5% of $[Fe^{III}(L^{1-H})][ClO_4]_2$ (low spin) dispersed in a lattice of $[Fe^{II}(L^1)][ClO_4]_2$ (low spin). This is perhaps not unreasonable given that $[Fe^{II}(L^1)]^{2+}$ and $[Fe^{III}(L^{1-H})]^{2+}$ would be expected to have very similar structures, not dissimilar molecular volumes, and would not be distinguishable from pure $[Fe^{II}(L^1)][ClO_4]_2$ using microanalytical data. In order to support this suggestion the X-band

**Table 2** Selected bond lengths (Å) and angles (°) in complexes **1**, **2** and **3**

| | **1** (M = Fe) | **2** (M = Ni) | **3** (M = Cu) |
|---|---|---|---|
| M(1)–N(1) | 2.102(3) | 2.087(5) | 2.218(9) |
| M(1)–N(2) | 2.101(3) | 2.088(4) | 2.024(9) |
| M(1)–N(3) | 2.112(3) | 2.083(5) | 2.193(8) |
| M(1)–N(4) | 2.099(3) | 2.083(5) | 2.211(9) |
| M(1)–N(5) | 2.113(3) | 2.116(5) | 2.081(9) |
| M(1)–N(6) | 2.092(3) | 2.089(5) | 2.032(8) |
| N(1)–M(1)–N(2) | 83.92(11) | 84.6(2) | 83.2(3) |
| N(1)–M(1)–N(3) | 83.30(11) | 84.6(2) | 80.8(3) |
| N(1)–M(1)–N(4) | 82.10(11) | 82.7(7) | 78.0(3) |
| N(1)–M(1)–N(5) | 164.24(12) | 165.9(2) | 161.6(3) |
| N(1)–M(1)–N(6) | 99.68(12) | 100.2(2) | 98.3(3) |
| N(2)–M(1)–N(3) | 84.30(11) | 85.6(2) | 84.5(3) |
| N(2)–M(1)–N(4) | 101.36(12) | 100.3(2) | 100.1(3) |
| N(2)–M(1)–N(5) | 81.15(12) | 82.4(2) | 83.8(3) |
| N(2)–M(1)–N(6) | 164.65(11) | 166.3(2) | 164.3(3) |
| N(3)–M(1)–N(4) | 163.66(12) | 165.5(2) | 157.6(3) |
| N(3)–M(1)–N(5) | 100.13(12) | 99.7(2) | 110.9(3) |
| N(3)–M(1)–N(6) | 81.34(11) | 82.1(2) | 80.9(3) |
| N(4)–M(1)–N(5) | 95.90(13) | 94.3(2) | 91.5(3) |
| N(4)–M(1)–N(6) | 93.93(12) | 93.2(2) | 95.1(3) |
| N(5)–M(1)–N(6) | 96.06(13) | 93.8(2) | 97.6(3) |

**Table 3** Mean Fe–N distances and spin states of a range of $FeN_6$ complexes

| Complex | Mean M–N/Å | Spin state | Ref. |
|---|---|---|---|
| $[Fe^{II}(tacn)_2]^{2+}$ | 2.03 | Low | 14 |
| $[Fe^{III}(tacn)_2]^{3+}$ | 1.99 | Low | 14 |
| $[Fe^{II}(L)]^{2+}$ | Not reported | High | 2(*b*) |
| $[Fe^{II}(L^1)]^{2+}$ | 2.10 | Low[a] | This work |
| $[Fe^{II}(en)_3]^{2+}$ | 2.23 | High | 15 |

[a] Contains ≈5% of low spin $[Fe^{III}(L^{1-H})]^{2+}$.

EPR spectrum of **1** in a frozen dimethylformamide glass was measured at 10 K (see ESI supplementary information). **1** (20 mg) was dissolved in degassed anhydrous DMF (1.0 ml) and the solution divided into two approximately equal portions. A drop of dimethylformamide containing a trace of triethylamine was added to one portion under aerobic conditions. The spectrum obtained for the initial (*i.e.* base free) solution was found to be rather low in intensity and to be typical of a low spin $d^5$ species with *g* values centred about that of the free electron. Low spin $d^5$ species would be expected to display a small Jahn–Teller distortion that explains a weak rhombicity observed in this spectrum. The spectrum of **1** in the presence of triethylamine

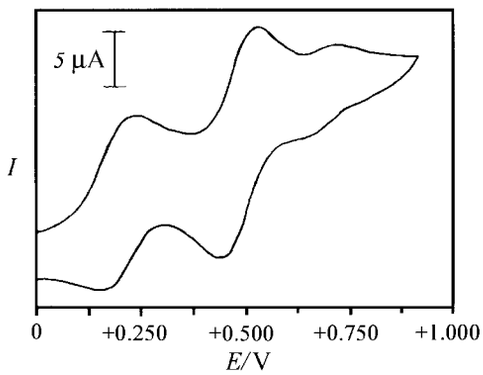


**Fig. 2** Cyclic voltammogram of $[Fe^{II}(L^1)][ClO_4]_2$ in 0.1 M $[n\text{-}Bu_4N]PF_6$ in acetonitrile *vs.* $Fc–Fc^+$.

indicated that the initial low spin iron(III) spectrum is only slightly altered but that a new feature centred at $g = 4.3$ appears. This latter signal is typical of that of a high-spin iron(III) complex. This seemingly contradictory result may be explained by considering that the addition of triethylamine is likely to generate the neutral tris-anilido species $[Fe^{III}(L^{1-3H})]^0$ [see ref. 2(c)]. Anilido ligands are strong σ and π donors and as such may be regarded as weak field ligands. Therefore the formation of a tris anilido species converts this system from a strong into a weak field case with a corresponding shift from low to high spin. These results corroborate the assignment of **1** as consisting of predominantly diamagnetic low spin $[Fe^{II}(L^1)][ClO_4]_2$ with a small amount of a low spin mono-anilido species $[Fe^{II}(L^{1-H})][ClO_4]_2$ present in the lattice. The above EPR results also imply that in the presence of base (and under aerobic conditions) there is an equilibrium between a range of $[Fe^{III}(L^{1-nH})]^{(3-n)+}$ species which vary in their degree of protonation and hence in spin state. In an additional experiment $[Fe^{III}(H_2O)_6][ClO_4]_3$ was added to $L^1$ dissolved in oxygenated DMF solution. An immediate deep blue coloration was observed ($\lambda = 710$ nm) and the EPR spectrum of this solution was found to be identical to that of $[Fe^{II}(H_2O)_6][ClO_4]_2$ prior to the addition of base. Subsequent addition of $Et_3N$ yielded a spectrum identical to that of $[Fe^{II}(H_2O)_6][ClO_4]_2$ basified under aerobic conditions. It seems likely that here the initial reaction yields $[Fe^{III}(L^{1-nH})]^{(3-n)+}$ type species in various degrees of protonation, and that addition of base again generates the neutral high spin complex $[Fe^{III}(L^{1-3H})]^0$. The blue coloration of single crystals of **1** can also be attributed to the presence of $[Fe^{III}(L^{1-H})]^{2+}$ if the strong absorption observed at 710 nm in solution is assigned as an anilido ligand-to-metal charge transfer band. Owing to its intensity this charge transfer band obscures the expected $^1T_{1g} \longleftarrow {}^1A_{1g}$ and $^1T_{2g} \longleftarrow {}^1A_{1g}$ transitions normally observed in low spin iron(II) species.

The electrochemical behaviour of $[Fe^{II}(L^1)][ClO_4]_2$ was measured by cyclic voltammetry (CV) in acetonitrile solution (Fig. 2). The complex displays two strong fully reversible oxidation processes at + 0.181 ($\Delta E_p = 60$ mV) and + 0.475 V ($\Delta E_p = 60$ mV) and weaker reversible processes at +0.695 V ($\Delta E_p = 72$ mV). The reductive electrochemistry proved to be complex with three irreversible oxidation processes occuring at −1.03, −1.585 and −1.906 V. The reversibility of the more prominent oxidation processes was confirmed by recording the CV data at a range of sweep rates. A plot of (sweep rate)$^{1/2}$ *vs.* cathodic current yielded a straight line, indicating truly reversible behaviour for each process. We can currently only speculate on the nature of the oxidised species although it seems likely that the first oxidative processes at + 0.181 V may be assigned to a metal based $Fe^{II} \longrightarrow Fe^{III}$ process. The other oxidations are presumably ligand based and may result in the generation of a ligand centred radical species. It is also possible that these oxidations involve concomitant deprotonation of the ligand to an anilido species.

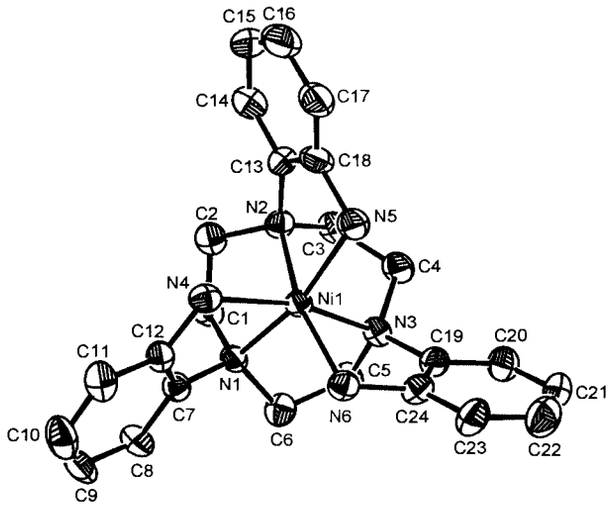


**Fig. 3** Ortep plot of $[Ni^{II}(L^1)]^{2+}$ **2** viewed normal to the plane defined by the macrocyclic donors. Other details as in Fig. 1.

To date all attempts at the preparation of $[Fe^{II}(L^1)][ClO_4]_2$, $[Fe^{III}(L^{1-H})][ClO_4]_2$ and $[Fe^{III}(L^{1-3H})]^0$ as discrete, analytically pure substances have failed.

**$[Ni^{II}(L^1)][ClO_4]_2$.** The single crystal structure of this material, which is isostructural to **1**, was obtained as shown in Fig. 3. The metal centre is six-co-ordinate with the macrocycle is in its typical face-capping mode and all three pendant aniline donors co-ordinated. The twist angle of the complex is 16° (octahedral twist angle = 0°) indicating that the bite angle of the *N*-2-aminophenyl pendant group is not sufficient to span two *cis* sites of an undistorted octahedron. The complex has no crystallographic symmetry but has approximate $C_3$ molecular symmetry. A comparison of the mean metal–ligand distances in $[Ni^{II}(L^1)]^{2+}$ (Ni–N 2.09 Å) to those of $[Ni^{II}(L)]^{2+}$ (Ni–N 2.16 Å)[2b] reveals a significantly stronger metal–ligand interaction in the case of $L^1$. In addition the metal–ligand distances are short in comparison to those of other nickel(II) hexaamine species contained in the Cambridge crystallography database.

The electronic spectrum of $[Ni^{II}(L^1)][ClO_4]_2$ was measured in acetonitrile solution (see ESI supplementary information for this spectrum and related $Ni^{II}N_6$ chromophores). Typically the ligand field splitting parameter $10Dq$ for octahedral nickel(II) complexes is given by the energy of the lowest $^3T_{2g} \longleftarrow {}^3A_{1g}$ transition, which in most cases is seen to consist of two components. For the purposes of calculating Δ in the cases of $[Ni^{II}(bipy)_3]^{2+}$ [16] and $[Ni^{II}(tacn)_2]^{2+}$ [17] the higher energy component has normally been assigned as the spin-allowed $^3T_{2g} \longleftarrow {}^3A_{1g}$ ($O_h$) transition, whilst the lower energy component is attributed to the spin-forbidden $^1E_g \longleftarrow {}^3A_{1g}$ transition. By following this convention a ligand field splitting value Δ of 12,330 cm$^{-1}$ and a Racah *B* parameter of 850 cm$^{-1}$ (as calculated from the $^3T_{2g} \longleftarrow {}^3A_{1g}$ and $^3T_{1g}(F) \longleftarrow {}^3A_{1g}$ transitions) is obtained for $[Ni^{II}(L^1)]^{2+}$. This value is significantly greater than that of the isoleptic complexes $[Ni^{II}(L)]^{2+}$ ($10Dq = 10{,}900$ cm$^{-1}$ [2b]) and $[Ni^{II}(en)_3]^{2+}$ indicating that the more rigid ligand enforces a stronger metal–ligand interaction. However Jørgensen[18] and Hancock and McDougall[19] have pointed out that the $^3T_{2g} \longleftarrow {}^3A_{1g}$ and $^1E_g \longleftarrow {}^3A_{1g}$ transitions are scrambled in complexes with $Dq/B$ values significantly greater than unity and therefore it not possible unequivocally to assign either component to a specific transition. In addition, for complexes in which there is a noted degree of trigonal distortion the lower energy band is also split into two components as seen in Gillum *et al.*'s analysis of the $[Ni^{II}\{(py)_3(tach)\}]^{2+}$ system ($(py)_3(tach)$ = *cis*,*cis*-1,3,5-tris{2-pyridylmethyleneamine}cyclohexane). In this case the $\{(py)_3(tach)]$ ligand was found to dictate almost perfect trigonal prismatic co-ordination geometry about $Ni^{II}$.[20]

**Table 4** Mean Ni–N distances and 10 *Dq* values of a range of $Ni^{II}N_6$ complexes

| Complex | Mean Ni–N/Å | $10Dq/cm^{-1}$ | Ref. |
|---|---|---|---|
| $[Ni^{II}(bipy)_3]^{2+}$ | 2.09 | 12,650 | 23, 24 |
| $[Ni^{II}(tacn)_2]^{2+}$ | 2.08 | 12,500, 12,350 | 25 |
| | | | 22 |
| $[Ni^{II}(L^1)]^{2+}$ | 2.09 | 12,330 | This work |
| $[Ni^{II}(L)]^{2+}$ | 2.16 | 10,900 | 2(*b*) |
| $[Ni^{II}(en)_3]^{2+}$ | 2.13 | 11,700 | 26, 18 |

The electronic spectra for the lower energy $T_{2g} \longleftarrow A_{1g}$ transition for $[Ni^{II}\{(py)_3(tach)\}]^{2+}$ and $[Ni^{II}(L^1)]^{2+}$ are very similar, and whilst simple model building studies indicate that $L^1$ will not support trigonal prismatic co-ordination geometry this observation implies that the rigorous assignment of the two components of the lower energy band is a non-trivial task.

The $10Dq$ value of $[Ni^{II}(L^1)]^{2+}$ is not very much smaller that of $[Ni^{II}(bipy)_3]^{2+}$ ($10Dq = 12{,}650$ $cm^{-1}$), which is the largest reported ligand-field splitting parameter for an octahedral nickel(II) species[21] (see Table 4). The high ligand-field splitting value in $[Ni^{II}(bipy)_3]^{2+}$ is partly due to the π acidity of the bipy ligand, but since $L^1$ may be described as a pure σ donor, steric factors must account for the high ligand field strengths observed. It is has been argued by Hancock that the high ligand field splitting value of $[Ni^{II}(tacn)_2]^{2+}$ (mean Ni–N distance 2.08 Å, $10Dq = 12{,}350$ $cm^{-1}$; note $10Dq$ values for this complex vary from author to author) is due to this complex having the minimum possible 'cage' size for nickel(II) cations and that the metal–ligand distances would be shorter were it not for the non-bonded repulsive interactions between pairs of methylene groups on adjacent macrocyclic rings.[22] In $L^1$ the 3 anilino donor groups (primary amino donors) would be expected to be sterically more efficient than an additional tacn moiety (secondary amino donors) and thus it appears that the rigidity of the pendant arms in $[Ni^{II}(L^1)]^{2+}$ prevents the closer approach of the anilino donor atoms to the metal centre and places it at a ligand field strength slightly less than that of $[Ni^{II}(tacn)_2]^{2+}$ and considerably higher than that of the more flexible tris chelates such as $[Ni(en)_3]^{2+}$ (mean N–Ni 2.13 Å, $\Delta = 11{,}700$ $cm^{-1}$).[18] An alternative way of stating this notion is that $L^1$ has an appropriate cavity size for the nickel(II) ion.

We speculated that a nickel(III) complex of $L^1$ might be accessible. However upon examination of the electrochemical behaviour of $[Ni^{II}(L^1)][ClO_4]_2$ only an irreversible oxidation at +1.05 V (*vs.* $Fc–Fc^+$) was observed.

**$[Cu^{II}(L^1)][ClO_4]_2$.** The above results suggest that $L^1$ permits the formation of six-co-ordinate $C_3$ symmetric complexes and that the ligand rigidity, to some extent, dictates the metal–ligand bond lengths. Copper(II) centres have a marked tendency to form five-co-ordinate complexes or six-co-ordinate Jahn–Teller distorted complexes, typically by elongation of one ligand–metal–ligand axis.[27] In an interesting example reported by Parker and co-workers it was shown that the Jahn–Teller distortion of copper(II) species can be suppressed in a $C_3$ symmetric tacn based system in which the pendant arm has the appropriate bite angle.[28] The ligand in this study was however a pendant arm phosphinic acid derivative and it could be argued that the stronger anionic ligand–metal interaction is partly responsible for dampening out of the Jahn–Teller distortion. We postulated that $L^1$ as a neutral, rigid $N_6$ donor would not permit the typical tetragonal distortion. Halcrow and co-workers have demonstrated that by using rigid sterically demanding ligands (3,3′-disubstituted 2,6-di(pyrazol-1-yl)-pyridines), compressed rhombic distortions may be promoted.[29] In this system three distinct axes were observed crystallographically with a mean Cu–N distance found to be 2.11 Å.

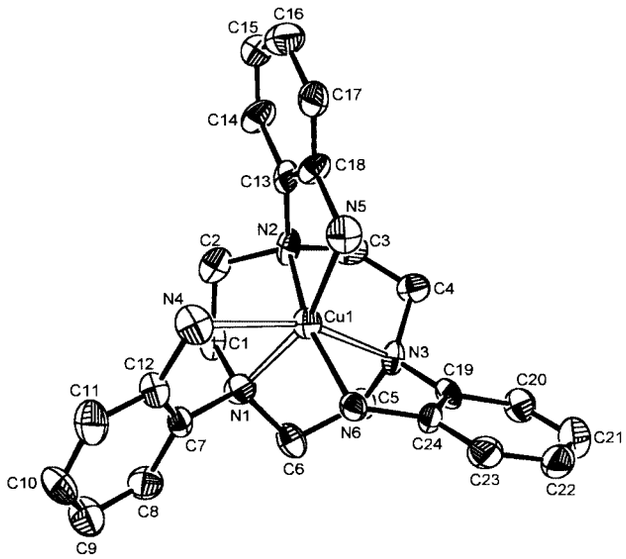


**Fig. 4** Ortep plot of $[Cu^{II}(L^1)]^{2+}$ **3** viewed normal to the plane defined by the macrocyclic donors. Other details as in Fig. 1.

The rhombic distortion was also confirmed spectroscopically (Q-band EPR).

The structure of the cation $[Cu^{II}(L^1)]^{2+}$ is illustrated in Fig. 4, with selected bond lengths and angles collected in Table 2. This complex also displays six-co-ordinate geometry with the macrocycle facially co-ordinated and all anilino donors bound to the metal centre. An examination of the metal–ligand bond lengths indicates that despite the high symmetry of the ligand three relatively short (Cu–N2, Cu–N5, Cu–N6) and three long (Cu–N1, Cu–N3, Cu–N4) metal–nitrogen distances are observed, indicating that the complex is rhombically, not tetragonally, distorted. The three axes are defined as *x* N3–Cu–N4 (long), *y* N1–Cu–N5 (intermediate) and *z* N2–Cu–N6 (short). It is worth noting that the two sets of short and long metal–ligand bond lengths are not restricted to those of macrocyclic donors and pendant-arm donors (which would maintain trigonal symmetry), but involve two pendant-arm donors and one macrocyclic donor and *vice versa*. The mean Cu–N distance is 2.12 Å, which is particularly short compared to related $CuN_6$ species in the Cambridge Crystallography database, indicating a compression of the metal–ligand bond lengths. The electronic spectrum of $[Cu^{II}(L^1)][ClO_4]_2$ in acetonitrile solution indicated a broad band at 695 nm ($\varepsilon = 107$ $dm^3$ $mol^{-1}$ $cm^{-1}$), $d_{x^2-y^2} \longleftarrow t_{2g}$) and a weaker broad feature at 1200 nm ($\varepsilon = 30$ $dm^3$ $mol^{-1}$ $cm^{-1}$ $d_{x^2-y^2} \longleftarrow d_{z^2}$), suggesting that the pseudo octahedral structure was maintained in solution. The presence of a near infrared band implies tetragonal distortion, although this distortion is not observed in the solid state structure. Similar observations were noted by Bernhardt and co-workers in the structure and electronic spectroscopy of the hexaamine cage complex $[Cu\{(NH_3)_2sar\}][NO_3]_4 \cdot H_2O$ (sar = 3,6,10,13,16,19-hexaazabicyclo[6.6.6]eicosane).[30] It should be noted that the mean Cu–N bond distance in the Cu–sar system is rather long at 2.17 Å and that ligand is likely to be more flexible than in the present case. It imposes trigonal symmetry but in this case an additional tetragonal elongation is also observed with a further small, but distinct, orthorhombic distortion. This latter distortion was evidenced by the observation of three distinct *g* values in the Q-band EPR spectrum. The X-band EPR of $[Cu^{II}(L^1)][ClO_4]_2$ doped into $[Zn^{II}(L^1)][ClO_4]_2$ measured at 100 K is shown in Fig. 5. The spectrum is essentially that of an axial $d^9$ species with $g_{\|} = 2.26$ ($A_{\|} = 147$ G) and $g_{\perp} = 2.058$ ($A_{\perp}$ = unresolved). The solution spectrum as measured in a frozen DMF–toluene glass was found be very similar with comparable *g* and *A* values. The shoulder to higher field on the perpendicular component may be interpreted as a so called "overshoot" feature resulting

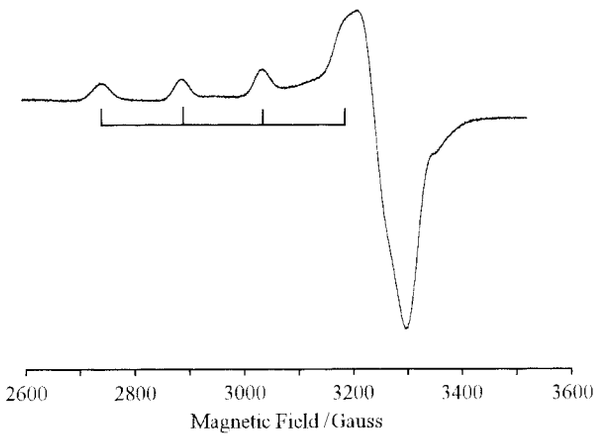


**Fig. 5** (a) X-Band EPR spectrum of $[Cu^{II}(L^1)][ClO_4]_2$ doped in $[Zn^{II}(L^1)][ClO_4]_2$ at 100 K.

from the relative magnitudes of the *g* and *A* anisotropies. Alternatively this may be interpreted as a rhombic feature. This system is currently the subject of an ENDOR and multi-frequency EPR study which will be described in a subsequent paper.

A plausible analysis for the distortion in $[Cu(L^1)]^{2+}$ may be made by noting that the co-ordination polyhedra as defined by the six nitrogen donor atoms of $[Fe(L^1)]^{2+}$, $[Ni(L^1)]^{2+}$ and $[Cu(L^1)]^{2+}$ are very similar with the mean M–N bond lengths spanning a narrow range (2.09–2.12 Å). Here it appears that by confining three donors within a macrocycle, and by having rigid aryl pendant arms bearing the remaining three donors, the degrees of torsional freedom available to the ligand are greatly restricted. As a final indicator of the inflexibility of $L^1$, the co-ordination geometry observed for $[Cu^{II}(L^1)]^{2+}$ is in contrast to that of $[Cu^{II}(L)]^{2+}$, with the latter complex found to be five-co-ordinate in the solid state with distorted square pyramidal geometry.[2b] In $[Cu^{II}(L)]^{2+}$ the additional methylene group between the pendant aniline and the macrocycle permits one of the pendant groups to rotate away from the metal centre to yield a five-co-ordinate metal centre. This is not possible in the case of $L^1$, in which rotation of the pendant arm about the N–Ar bond results in an unfavourable steric interaction of the pendant amine group and the macrocyclic methylene residues.

**$[Zn^{II}(L^1)][ClO_4]_2$ 4.** Reaction of $L^1$ with $Zn(ClO_4)_2{\cdot}6H_2O$ in refluxing ethanol afforded $[Zn^{II}(L^1)][ClO_4]_2$ **4** as colourless microcrystals. Despite repeated attempts, crystals of $[Zn^{II}(L^1)][ClO_4]_2$ failed to yield workable X-ray crystallographic data. The $^1$H NMR spectrum of the complex in acetonitrile solution indicated that it is $C_3$ symmetric in solution. All three aromatic pendant groups are equivalent and the macrocyclic methylene groups have been resolved into two complex multiplets at $\delta$ 3.60 and 2.99. These latter resonances are tentatively assigned as due to *endo*- and *exo*- protons of the macrocyclic chelate rings. The pendant aniline $NH_2$ groups in the "free" ligand occur as a broad singlet at $\delta$ 4.17 (in $CD_3CN$ solution) and shift to a broad singlet at $\delta$ 4.56 upon co-ordination. This implies that in solution all six *N*-donors are co-ordinated. The $^1$H NMR was found not to change significantly when recorded over the temperature range of −40 to +70 °C. This observation suggests that over the experimental temperature range the $[Zn^{II}(L^1)]^{2+}$ cation is non-fluxional in solution. This is in contrast to the behaviour of $[Zn^{II}(L)]^{2+}$ which displayed a complex, temperature-dependant NMR spectrum.[2a] Again it can be seen that the larger pendant chelate rings of $L^1$ permit greater torsional flexibility in the co-ordinated ligand system.

## Acknowledgements

We wish to thank the Engineering and Physical Sciences Research Council (EPSRC) for financial support, and the EPSRC Mass Spectrometry Service (Swansea, UK) for valuable experimental assistance. We would also like to thank Dr Angelo J. Amoroso (Cardiff), Dr Athanasia Dervisi (Cardiff) and Professor Andrew Harrison (Edinburgh) for valuable discussion.

## References

1 P. Chaudhuri and K. Wieghardt, *Prog. Inorg. Chem.*, 1987, **35**, 329; P. V. Bernhardt and G. A. Lawrance, *Coord. Chem. Rev.*, 1990, **104**, 297; K. P. Wainwright, *Coord. Chem. Rev.*, 1997, **35**, 166.
2 (*a*) O. Schlager, K. Wieghardt, H. Grondey, A. RufiÕska and B. Nuber, *Inorg. Chem.*, 1995, **34**, 6440; (*b*) O. Schlager, K. Wieghardt and B. Nuber, *Inorg. Chem.*, 1995, **34**, 6449; (*c*) O. Schlager, K. Wieghardt and B. Nuber, *Inorg. Chem.*, 1995, **34**, 6456.
3 T. Koike, T. Gotoh, A. Aoki, E. Kimura and M. Shiro, *Inorg. Chim. Acta*, 1998, **270**, 424.
4 (*a*) L.-S. Choi and G. E. Collins, *Chem. Commun.*, 1998, 893; (*b*) G. E. Collins, L. S. Choi and J. H. Callahan, *J. Am. Chem. Soc.*, 1998, **120**, 1474.
5 For recent examples see: B. Albela, E. Bill, O. Brosch, T. Weyhermüller and K. Wieghardt, *Eur. J. Inorg. Chem.*, 2000, 139; M. Di Vaira, F. Mani and P. Stoppioni, *Inorg. Chim. Acta*, 2000, **297**, 61; S. J. Brudenell, L. Spiccia, A. M. Bond, G. D. Fallon, D. C. R. Hockless, G. Lazarev, P. J. Mahon and E. R. T. Tiekink, *Inorg. Chem.*, 2000, **39**, 881; L. M. Berreau, J. A. Halfen, V. G. Young, Jr. and W. B. Tolman, *Inorg. Chim. Acta*, 2000, **297**, 115; J. Müller, A. Kikuchi, E. Bill, T. Weyhermüller, P. Hiderbrandt, L. Ould-Moussa and K. Wieghardt, *Inorg. Chim. Acta*, 2000, **297**, 265; M. Di Vaira, F. Mani and P. Stoppioni, *Eur. J. Inorg. Chem.*, 1999, 833; T. Glaser, F. Kesting, T. Beissel, E. Bill, T. Weyhermüller, W. Meyer-Klaucke and K. Wieghardt, *Inorg. Chem.*, 1999, **38**, 722; T. Glaser, E. Bill, T. Weyhermüller, W. Meyer-Klaucke and K. Wieghardt, *Inorg. Chem.*, 1999, **38**, 2632; B. Albela, E. Bothe, O. Brosch, K. Mochiazuki, T. Weyhermüller and K. Wieghardt, *Inorg. Chem.*, 1999, **38**, 5131; R. Schnepf, A. Sololowski, J. Müiller, V. Bachier, K. Wieghardt and P. Hildebrandt, *J. Am. Chem. Soc.*, 1998, **120**, 2352; F. N. Penkert, T. Weyhermüller and K. Wieghardt, *Chem. Commun.*, 1998, 557; H. Weller, T. A. Kaden and G. Hopfgarten, *Polyhedron*, 1998, **17**, 4543; M. Koikawa, K. B. Jensen, H. Matsushima, T. Tokii and H. Toflund, *J. Chem. Soc.*, *Dalton Trans.*, 1998, 1085; M. Di Vaira, F. Mani and P. Stoppioni, *J. Chem. Soc.*, *Dalton Trans.*, 1998, 3209; S. J. Brudenell, L. Spiccia, A. M. Bond, P. C. Mahon and D. C. R. Hockless, *J. Chem. Soc.*, *Dalton Trans.*, 1998, 3919; A. Sokolowski, B. Adam, T. Weyhermüller, A. Kikuchi, K. Hildenbrand, R. Schnepf, P. Hildebrandt, E. Bill and K. Wieghardt, *Inorg. Chem.*, 1997, **36**, 3702; B. Adam, E. Bill, E. Bothe, B. Goerdt, G. Haselhorst, K. Hildenbrand, A. Sokolowski, S. Steenken, T. Weyhermüller and K. Wieghardt, *Chem. Eur. J.*, 1997, **3**, 308; M. Di Vaira, F. Mani and P. Stoppioni, *J. Chem. Soc.*, *Dalton Trans.*, 1997, 1375; T. Beissel, F. Birkelbach, E. Bill, T. Glaser, F. Kesting, C. Krebs and K. Wieghardt, *J. Am. Chem. Soc.*, 1996, **118**, 12376.
6 D. A. House, in *Comprehensive Co-ordination Chemistry*, eds. G. Wilkinson, R. D. Gillard and J. A. McCleverty, Pergamon Press, Oxford, 1987, vol. 2, p. 59.
7 D. R. Marks, D. J. Phillips and J. P. Redfern, *J. Chem. Soc. A*, 1967, 1464.
8 G. J. Grant and D. J. Royer, *J. Am. Chem. Soc.*, 1981, **103**, 867.
9 K. Wieghardt, W. Schmidt, B. Nuber and J. Weiss, *Chem. Ber.*, 1979, **112**, 2220.
10 D. D. Perrin and W. F. A. Amarego, *Purification of Laboratory Chemicals*, Pergamon, Oxford, 1988.
11 G. M. Sheldrick, *Acta Crystallogr.*, *Sect. A*, 1990, **46**, 467.
12 G. M. Sheldrick, SHELXL 96, Program for Crystal Structure Refinement, University of Göttingen, 1996.
13 Ortep 3 for Windows, A Version of ORTEP III with a Graphical User Interface (GUI), L. J. Farrugia, *J. Appl. Crystallogr.*, 1997, **30**, 565.
14 J. C. A. Boeyens, A. G. S. Forbes, R. D. Hancock and K. Wieghardt, *Inorg. Chem.*, 1985, **24**, 19226.
15 J. Li, Z. Chen, J. J. Emge and D. M. Proserpio, *Inorg. Chem.*, 1997, **36**, 1437.
16 R. A. Palmer and T. S. Piper, *Inorg. Chem.*, 1966, **5**, 864.
17 L. J. Zompa, *Inorg. Chem.*, 1978, **17**, 2531.
18 C. K. Jørgensen, *Acta Chem. Scand.*, 1955, **9**, 1362.
19 R. D. Hancock and G. J. McDougall, *J. Chem. Soc.*, *Dalton Trans.*, 1977, 67.

20 W. O. Gillum, R. A. D. Wentworth and R. P. Childers, *Inorg. Chem.*, 1970, **9**, 1825.
21 A. B. P. Lever, *Inorganic Electronic Spectroscopy*, Elsevier, Amsterdam, 1984, p. 508.
22 V. J. Thom, G. J. McDougall, J. C. A. Boeyens and R. D. Hancock, *J. Am. Chem. Soc.*, 1984, **106**, 3198; R. D. Hancock, *Prog. Inorg. Chem.*, 1989, **37**, 187.
23 C. K. Jørgensen, *Adv. Chem. Phys.*, 1963, **5**, 33.
24 D. J. Chestnut, R. C. Haushalter and J. Zubieta, *Inorg. Chim. Acta*, 1999, **292**, 41.
25 L. J. Zompa and T. N. Margulis, *Inorg. Chim. Acta*, 1980, **45**, L263.
26 J. D. Korp, I. Bernal, R. A. Palmer and J. C. Robinson, *Acta Crystallogr.*, *Sect. B*, 1980, **36**, 560.
27 B. N. Figgis and M. A. Hitchman, *Ligand Field Theory Theory and Applications*, Wiley, New York, 2000, p. 298; C. E. Holloway and M. Melnik, *Rev. Inorg. Chem.*, 1995, **15**, 147; E. I. Solomon and A. B. P. Lever, *Inorganic Electronic Structure and Spectroscopy*, Wiley, New York, 1999, vol. II, p. 76; M. Milnik, M. Kabesova, L. Macaskova and C. E. Holloway, *J. Coord. Chem.*, 1998, **45**, 31; L. R. Falvello, *J. Chem. Soc.*, *Dalton Trans.*, 1997, 4463; B. J. Hathaway, in *Comprehensive Co-ordination Chemistry*, eds. G. Wilkinson, J. McCleverty and R. D. Gillard, Pergamon, Oxford, 1987, vol. 5, p. 610.
28 E. Cole, D. Parker, G. Ferguson, J. F. Gallagher and B. Kaitner, *J. Chem. Soc.*, *Chem. Commun.*, 1991, 1473.
29 N. K. Solanki, E. J. McInnes, F. E. Mabbs, S. Radojevic, M. McPartlin, N. Feeder, J. E. Davies and M. A. Halcrow, *Angew. Chem.*, *Int. Ed.*, 1998, **37**, 2221.
30 P. V. Bernhardt, R. Bramley, L. M. Engelbrandt, J. M. Harrowfield, D. C. R. Hockless, B. R. Korybut-Daszkiewicz, E. R. Krause, T. Morgan, A. M. Sargeson, B. W. Skelton and A. H. White, *Inorg. Chem.*, 1995, **34**, 3589.